

Nuclear-Structure Studies of Sr⁸⁸ and Y⁸⁹ by Inelastic Alpha-Particle Scattering*

J. ALSTER,† D. C. SHREVE, AND R. J. PETERSON‡

Physics Department, University of Washington, Seattle, Washington

(Received 12 November 1965)

The inelastic scattering of 42-MeV alpha particles from Sr⁸⁸ and Y⁸⁹, was studied in order to test the validity of the weak-coupling core-excitation model for these nuclei and to obtain an angular distribution for the excitation of the $g_{9/2}$ single-particle state at 0.906 MeV in Y⁸⁹. Angular distributions were obtained for scattering to the ground state and the 1.84-MeV (2^+), 2.74-MeV (3^-), and 3.21-MeV (2^+) states in Sr⁸⁸; and to the ground state and the 0.906-MeV ($\frac{3}{2}^+$), 1.51-MeV ($\frac{3}{2}^-$), 1.75-MeV ($\frac{5}{2}^-$), 2.22-MeV ($\frac{3}{2}^+$), 2.53-MeV ($\frac{7}{2}^+$), 2.84-MeV, and 3.1-MeV states in Y⁸⁹. The phase rule was used to obtain parities for additional levels in Y⁸⁹ at 3.70, 3.98, and 4.17 MeV. A parametrized phase-shift analysis was used to fit the elastic-scattering data, and the Austern-Blair model with the same parameters was used to extract values of $\beta_1 R$ from the inelastic angular distributions. It is shown that the weak-coupling model is not a good description for the excited states of Y⁸⁹. A shell-model calculation correlating the differential cross sections to the 2^+ states in Sr⁸⁸ and the 1.51- and 1.75-MeV states in Y⁸⁹ is made, and the results are found to be in slightly better agreement with experiment. The differential cross section to the 0.906-MeV ($g_{9/2}$) single-particle state is in agreement with the Austern-Blair model for an $I=5$ transition.

I. INTRODUCTION

THE study of the inelastic scattering of medium energy alpha particles has proved to be a powerful tool in the nuclear spectroscopy of low-lying collective levels.¹⁻³ Spin and parity assignments as well as transition strengths, which can be related to electromagnetic transition rates,⁴ have been extracted from the shapes and magnitudes of the angular distributions.⁵ With the advent of high-resolution solid-state detectors, it has been possible to extend this type of investigation from even-even nuclei to even-odd nuclei where the relatively high density of states at low excitation energies had hitherto prevented the study of individual states.

An investigation of the inelastic scattering of alpha particles from Sr⁸⁸ and Y⁸⁹ is of special interest for several reasons. It is of interest to obtain a measure of the excitation of single-particle states with inelastic scattering of strongly absorbed particles since it has almost always been assumed that these projectiles would mainly excite collective states.⁵ No angular distribution measurements for the excitation of unambiguous single-particle states by inelastic alpha-particle scattering have been reported. The first excited state in Y⁸⁹ is a single-particle state corresponding to the promotion of the unpaired $2p_{1/2}$ proton in the ground state to the $1g_{9/2}$ subshell,⁵ and a study of the angular distribution for this state should therefore prove to be

valuable in the understanding of the mechanism of alpha-particle scattering.

Further, Shafroth *et al.*⁶ had proposed that several of the states in Y⁸⁹ might be explained in terms of the weak-coupling core-excitation model.⁷ This model assumes that the unpaired $2p_{1/2}$ proton of Y⁸⁹ interacts only weakly with the Sr⁸⁸ core and its collective excitations. If this assumption is valid, one should expect pairs of states in Y⁸⁹ of spin and parity corresponding to the coupling of the $2p_{1/2}$ proton to each excited state of the Sr⁸⁸ core at energies given by the center of gravity theorem.⁷

It was proposed that the 1.51-MeV ($\frac{3}{2}^-$) and 1.75-MeV ($\frac{5}{2}^-$) states in Y⁸⁹ correspond to the 1.84-MeV (2^+) state in Sr⁸⁸, the 2.22- and 2.53-MeV states in Y⁸⁹ to the 2.74-MeV (3^-) state in Sr⁸⁸, and the 2.84- and 3.1-MeV states in Y⁸⁹ to the 3.21-MeV (2^+) state in Sr⁸⁸.⁸ The discrepancy of the positions of the states in Y⁸⁹ from those given by the center of gravity theorem is not serious.

Because alpha particles preferentially excite collective levels, one should excite mainly those states in Y⁸⁹ that correspond to the collective excitations of the Sr⁸⁸ core. The differential cross sections for the inelastic scattering of alpha particles exciting the states in Y⁸⁹ are then related to the differential cross section of the corresponding state in Sr⁸⁸ by the equation⁵

$$\frac{d\sigma}{d\Omega} \text{Y}^{89}(\frac{1}{2} \rightarrow J_f) = \frac{(2J_f+1)}{(2J_c+1)(2 \times \frac{1}{2} + 1)} \frac{d\sigma}{d\Omega} \text{Sr}^{88}(0 \rightarrow J_c), \quad (1)$$

where J_f is the spin of the excited state in Y⁸⁹ and J_c is the spin of the related state in Sr⁸⁸. In particular, this equation and the identifications of Shafroth *et al.*⁶ lead to the prediction that the sum of the differential

* Work performed under the auspices of the U. S. Atomic Energy Commission.

† Present address: Physics Department, Northeastern University, Boston, Massachusetts.

‡ National Science Foundation Predoctoral Fellow.

¹ D. K. McDaniels, J. S. Blair, S. W. Chen, and G. W. Farwell, Nucl. Phys. **17**, 614 (1960).

² R. Beurtey, P. Catillon, R. Chaminade, M. Crut, H. Faraggi, A. Papineau, J. Saudinos, and J. Thirion, Compt. Rend. **252**, 1756 (1961).

³ H. W. Broek, Phys. Rev. **130**, 1914 (1963).

⁴ W. T. Pinkston and G. R. Satchler, Nucl. Phys. **27**, 270 (1961).

⁵ J. S. Blair, Argonne National Laboratory Report No. ANL-6878, 1964 (unpublished).

⁶ S. M. Shafroth, P. N. Trehan, and D. M. Van Patter, Phys. Rev. **129**, 704 (1963).

⁷ A. de-Shalit, Phys. Rev. **122**, 1530 (1961); A. Braunstein and A. de-Shalit, Phys. Letters **1**, 264 (1962).

⁸ S. Shastri and R. Bhattacharyya, Nucl. Phys. **55**, 397 (1964).

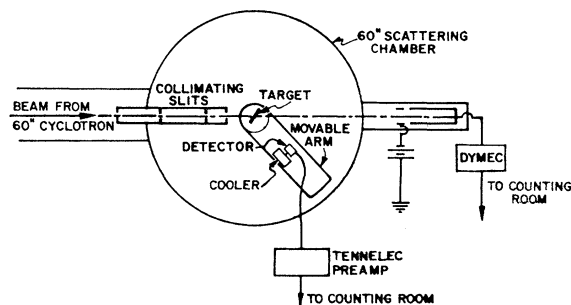


FIG. 1. Plan of scattering area showing relative positions of scattering chamber, detectors, and associated equipment.

cross sections to the 1.51-MeV ($\frac{3}{2}^-$) and 1.75-MeV ($\frac{5}{2}^-$) states in Y^{89} should equal the differential cross section for the 1.84-MeV (2^+) state in Sr^{88} , the sum of the differential cross sections for the 2.22-MeV ($\frac{5}{2}^+$) and 2.53-MeV ($\frac{7}{2}^+$) should equal the differential cross section for the 2.74-MeV (3^-) state in Sr^{88} , and the sum of the differential cross sections to the 2.84- and 3.1-MeV states should equal the differential cross section for the 3.21-MeV state in Sr^{88} . Also implicit is the prediction that the angular distributions for the excitation of the states in Y^{89} should be the same as that for the related state in Sr^{88} .

The core-excitation model has recently been applied to inelastic scattering from various nuclei with varying degrees of success. The first such work was the study of the Ni^{62} - Cu^{63} pair, where quadruplets of states in Cu^{63} were ascribed to states in Ni^{62} .⁹ It has recently been shown, however, that the model is too simple a description for these nuclei.¹⁰

The study of $N^{15}(\alpha, \alpha')$ and $O^{16}(\alpha, \alpha')$ has shown¹¹ that a pair of states in N^{15} might be described as the coupling of a $1p_{1/2}$ proton hole to the $3^-(6.14\text{-MeV})$ octupole state in O^{16} . Also, investigations of the $Al^{27}(\alpha, \alpha')$ and $Si^{28}(\alpha, \alpha')$ reactions have shown¹² that five of the states in Al^{27} might correspond to the coupling of a $d_{5/2}$ proton hole to the 2^+ excited state of Si^{28} . The low-lying states of Au^{197} have been described as couplings of a $2d_{3/2}$ proton to a 2^+ excited state of the Pt^{196} core.^{13,7}

Possibly the best example of core excitation, however, is the coupling of the $1g_{9/2}$ proton in Bi^{209} and the $3p_{1/2}$ neutron hole in Pb^{207} to the $3^-(2.615\text{-MeV})$ state in Pb^{208} as shown by $Pb^{207}(\alpha, \alpha')$, $Pb^{208}(\alpha, \alpha')$, and $Bi^{209}(\alpha, \alpha')$ experiments.¹⁴

⁹ G. Bruge, J. C. Faivre, M. Barloutaud-Crut, H. Faraggi, and J. Saudinos, *Phys. Letters* **7**, 203 (1963).

¹⁰ A. G. Blair, *Phys. Letters* **9**, 37 (1964).

¹¹ A. Bussiere, N. K. Glendenning, B. G. Harvey, J. Mahoney, and J. R. Meriwether, *Phys. Letters* **16**, 296 (1965).

¹² J. Kokame, K. Fukunaga, and H. Nakamura, *Phys. Letters* **14**, 234 (1965).

¹³ A. de-Shalit, *Phys. Letters* **15**, 170 (1965).

¹⁴ J. Alster, *Phys. Rev.* (to be published); *Proceedings of the Congrès International de Physique Nucléaire, II*, edited by P. Gungenberger (CNRS, Paris, 1964), p. 450.

A possible alternative description of the states at 1.51 and 1.75 MeV in Y^{89} is that they are simple shell-model configurations. It is well known that the ground and first excited states of Y^{89} are described as single $p_{1/2}$ and $g_{9/2}$ proton orbitals, respectively, outside the closed Sr^{88} core and that the ground state of Zr^{90} involves a linear combination of $(p_{1/2})^2$ and $(g_{9/2})^2$ configurations.¹⁵⁻¹⁷ Inspection of the energy levels of shell-model orbitals suggests that the next simplest configurations in Y^{89} correspond to $2p_{3/2}$ and $1f_{5/2}$ proton holes in the Zr^{90} ground-state configuration and that these configurations are the main components of the 1.51- and 1.75-MeV states. A similar shell-model description may be invoked for the lowest 2^+ levels of Sr^{88} , namely that the leading components of these states are the proton $2p_{1/2}-1f_{5/2}$ and $2p_{1/2}-2p_{3/2}$ particle-hole configurations. Introduction of such model wave functions into distorted-wave Born approximation (DWBA) calculations of inelastic-scattering cross sections leads to definite predictions for the ratios and absolute magnitudes of the cross sections. Comparison between these calculations and the experimental results will be given in Sec. V.

II. EXPERIMENTAL PROCEDURE

The 42-MeV α -particle beam from the University of Washington 60-in. cyclotron was focused and energy analyzed by a pair of magnets and directed into a 60-in. scattering chamber. The beam size was defined by a pair of slits $\frac{1}{16}$ in. wide and $\frac{1}{4}$ in. high separated by 12 in.

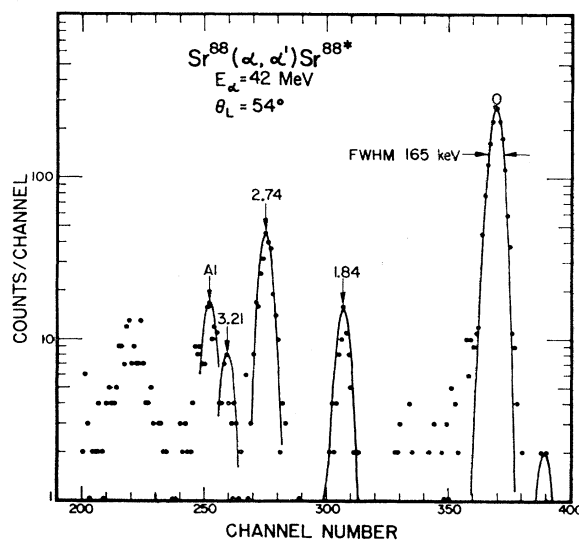


FIG. 2. Pulse-height spectrum of 42-MeV alpha particles scattered from Sr^{88} . The excitation energies of the states studied are listed above their respective peaks. The solid curves are Gaussian distributions and serve only to guide the eye.

¹⁵ J. L. Yntema, *Phys. Letters* **11**, 140 (1964).

¹⁶ B. Bayman, A. S. Reiner, and R. K. Sheline, *Phys. Rev.* **115**, 1627 (1959).

¹⁷ S. Cohen, R. D. Lawson, M. H. MacFarlane, and M. Soga, *Phys. Letters* **10**, 195 (1964).

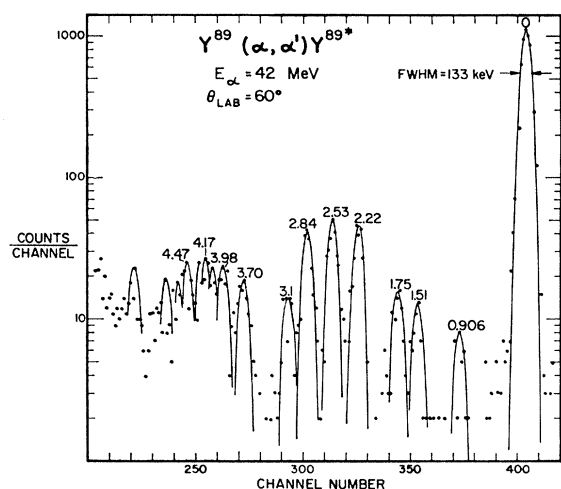


FIG. 3. Pulse-height spectrum of 42-MeV alpha particles scattered from Y^{89} . The excitation energies of the states studied are listed above their respective peaks. The solid curves are Gaussian distributions and serve only to guide the eye.

After passing through the target at the center of the chamber the beam was collected in a Faraday cup equipped with a secondary electron suppressor. The collected charge was measured by scaling the output of a charge integration unit which produced a standard pulse for every 10^{-11} C of charge collected.¹⁸ (See Fig. 1.)

Fragile but self-supported foils of Sr^{88}O approximately 0.8 mg/cm^2 thick were obtained by reducing $\text{Sr}^{88}\text{CO}_3$, enriched to 99%,¹⁹ to the metal with subsequent vacuum evaporation. This method of target preparation is fully described elsewhere.²⁰ The Y^{89} targets consisted of rolled foils of isotopically pure Y metal approximately 0.9 mg/cm^2 thick.²¹

Cooled Li-drifted silicon detectors were used as particle detectors. The electronic system consisted of Tennelec preamplifiers, RIDL biased amplifiers, and a 512 channel nuclear data multichannel analyzer. The multichannel analyzer was gated with a trigger pulse from the output of the biased amplifier. This pulse was also fed to a scaler and compared to a scaler counting the actual number of pulses analyzed by the multichannel analyzer. The ratio of the readings of the two scalers gave a direct measure of the dead time correction for the multichannel analyzer. The energy calibration of the whole system was determined from the elastic scattering of α particles from Au, O, and C at several angles. The over-all energy spread was approximately 130 keV for the Y^{89} and ranged from 150 to 170 keV for Sr^{88} because of holes in the Sr^{88} target.

For Sr^{88} the elastic-scattering data were taken at 1-deg intervals, from 12 to 36 deg, and in 2-deg in-

tervals, from 36 to 82 deg. Angular distributions to the excited states were measured from 20 to 82 deg in 2-deg intervals. Typical energy spectra for 42-MeV α particles scattered from Sr^{88} and Y^{89} are shown in Figs. 2 and 3. Oxygen and carbon were serious impurities in both targets. At angles (less than 45 deg) where peaks in the energy spectrum were obscured by these contaminants no effort was made to extract cross sections, which resulted in gaps in our experimental angular distributions. A slight Al contamination in the Sr^{88} target could be corrected for since the scattering of 42-MeV α particles from Al had been measured previously in this laboratory.²²

The relative errors for the Y^{89} data were $\pm 5\%$, because of systematic errors in the normalization of data taken at different times. The absolute error is approximately $\pm 8\%$. Since no target thickness measurement could be made of extremely fragile SrO target, the Sr^{88} differential cross sections were normalized by assuming that the ratio of the elastic cross section to the Rutherford cross section at small angles is the same for Sr^{88} and Y^{89} . This procedure adds an estimated $\pm 5\%$ error to the absolute differential cross sections for Sr^{88} . The additional relative errors in Sr^{88} are the same as for Y^{89} .

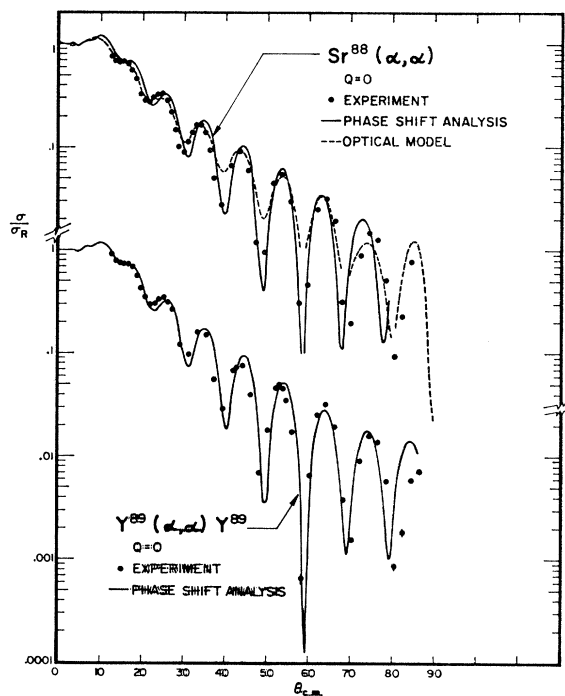


FIG. 4. Differential cross sections divided by the Rutherford cross sections of 42-MeV alpha particles for the elastic scattering from Sr^{88} and Y^{89} . The solid curves are the results of the parameterized phase-shift calculations using the parameters given in Table III. The dashed curve is the result of an optical model calculation using the parameters $V = -50 \text{ MeV}$, $W = -20 \text{ MeV}$, $R = 7.038 \text{ F}$ and $D = 0.50 \text{ F}$.

¹⁸ DYMEC 2211 voltage-to-frequency converter, Hewlett-Packard, Inc., Palo Alto, California.

¹⁹ Obtained from Oak Ridge National Laboratory, Isotopes Sales Division.

²⁰ J. Sauer, Rev. Sci. Instr. 36, 1374 (1965).

²¹ Obtained from F. Karasek, Argonne National Laboratory.

²² I. Naqib, Ph.D. thesis, University of Washington, 1962 (unpublished).

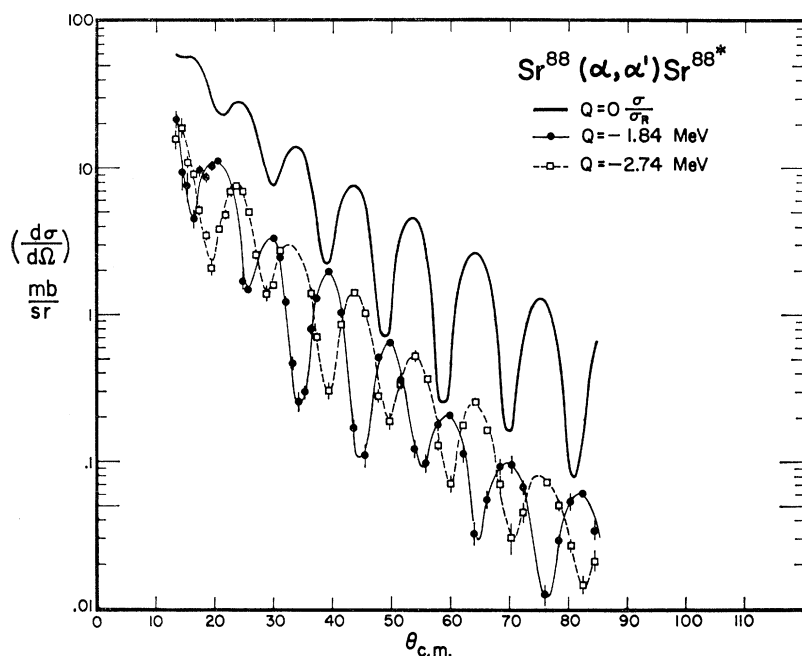


FIG. 5. Angular distributions for 42-MeV alpha particles exciting the 1.84- and 2.74-MeV states in Sr^{88} . The ratio of elastic to Rutherford cross sections is shown for comparison. Errors shown are statistical in nature and are shown whenever they exceed the point size. The curves are shown to guide the eye.

III. EXPERIMENTAL RESULTS

The measured values of the elastic differential cross sections divided by the Rutherford cross sections for Sr^{88} and Y^{89} are given in Table I and are also shown in Fig. 4. Figure 5 shows the inelastic differential cross sections for the excitation of the 1.84- and 2.74-MeV states in Sr^{88} . The ratio of the elastic differential cross section to the Rutherford cross section for Sr^{88} is also shown for comparison. The angular distributions for

the excitation of the 0.906-, 2.22-, and 2.53-MeV states of Y^{89} are shown in Fig. 6, the 1.51- and 1.75-MeV states in Fig. 7, the 2.84- and 3.1-MeV states in Fig. 8, and the 3.70-, 3.98-, and 4.17-MeV states in Fig. 9. In each of the Figs. 6, 7, 8, and 9, the ratio of the elastic differential cross section to the Rutherford cross section for Y^{89} is shown for comparison. The 3.21-MeV (2^+) state in Sr^{88} was only weakly excited and could not be consistently extracted from the background (mainly because of the tail from the strongly excited 2.74-MeV

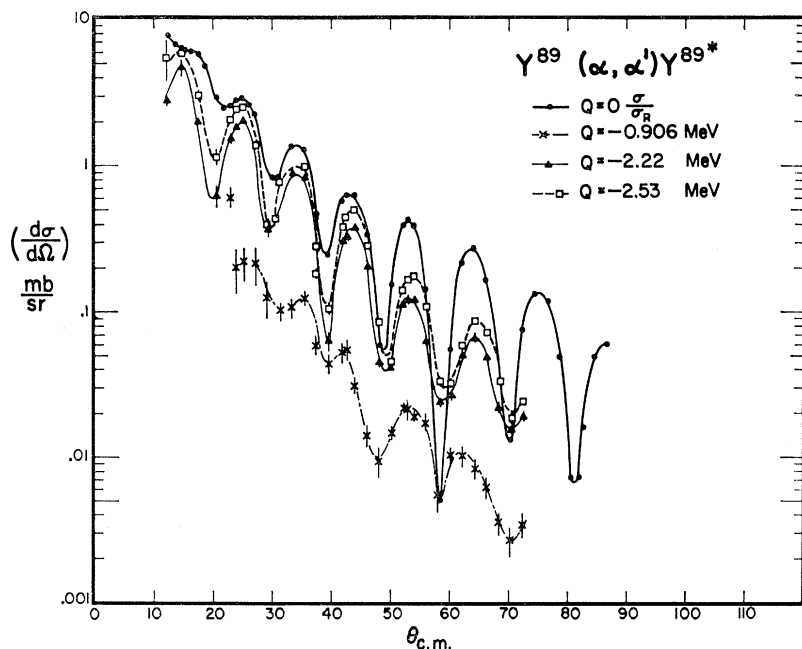


FIG. 6. Angular distributions for 42-MeV alpha particles exciting the 0.906-, 2.22-, and 2.53-MeV states in Y^{89} . The ratio of elastic to Rutherford cross sections is shown for comparison. Errors shown are statistical in nature and are shown whenever they exceed the point size. The curves are shown to guide the eye.

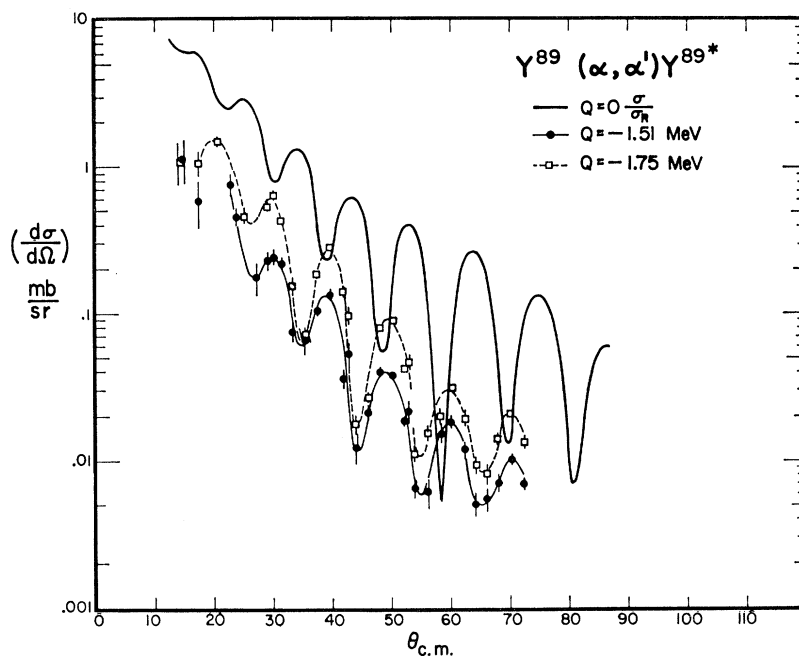


FIG. 7. Angular distributions for 42-MeV alpha particles exciting the 1.51- and 1.75-MeV states in Y⁸⁹. The ratio of elastic to Rutherford cross sections is shown for comparison. Errors shown are statistical in nature and are shown whenever they exceed the point size. The curves are shown to guide the eye.

state). Its angular distribution is not shown and only an upper limit for the value of $(\beta_2 R)^2$ (see Sec. VI) could be extracted.

Several important points should be made about the angular distributions to the states in Y⁸⁹. First, the angular distribution for the 0.906-MeV ($g_{9/2}$) single-particle state (Fig. 6) looks very similar to the angular distributions for the collective states. In particular, it

has oscillations in phase with the elastic angular distribution in agreement with the phase rule for a parity changing transition,²³ and the envelope of the angular distribution decreases at the same rate as those for the collective $I=3$ transitions. (Unfortunately, the shape of the angular distribution could not be extracted from the data below 20 deg because of the oxygen and carbon contaminations.)

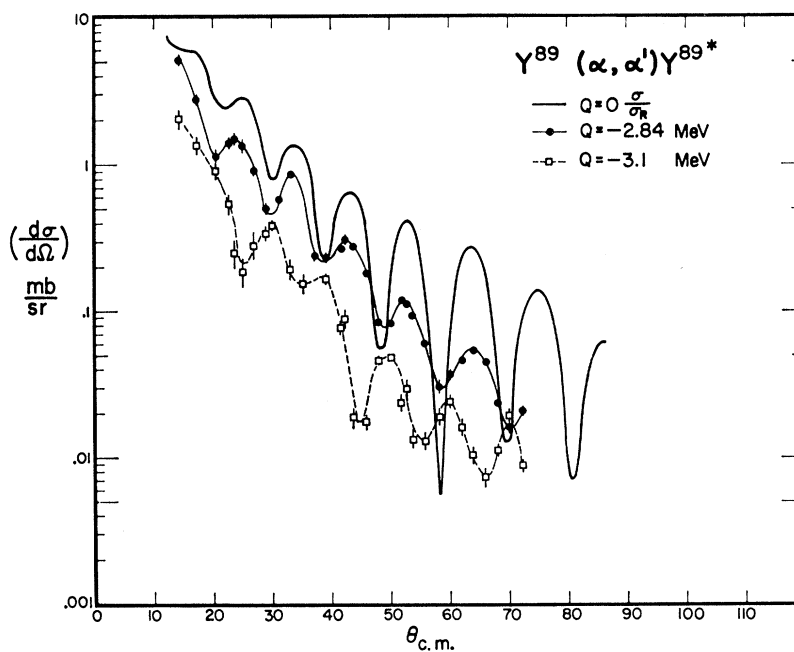


FIG. 8. Angular distributions for 42-MeV alpha particles exciting the 2.84- and 3.1-MeV states in Y⁸⁹. The ratio of elastic to Rutherford cross sections is shown for comparison. Errors shown are statistical in nature and are shown whenever they exceed the point size. The curves are shown to guide the eye.

²³ J. S. Blair, Phys. Rev. **115**, 928 (1959).

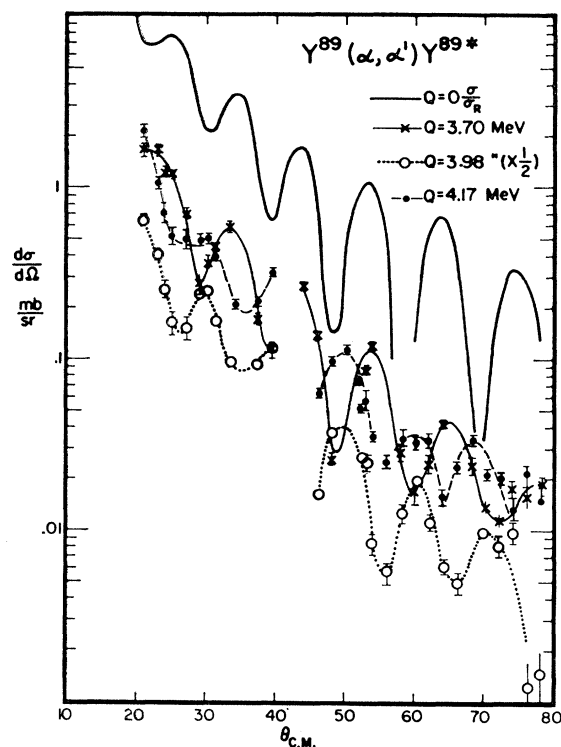


FIG. 9. Angular distributions for 42-MeV alpha particles exciting the 3.70-, 3.98-, and 4.17-MeV states in Y^{89} . The ratio of elastic to Rutherford cross sections is shown for comparison. Errors shown are statistical in nature and are shown whenever they exceed the point size. The curves are shown to guide the eye.

Second, the angular distribution for the 2.84-MeV state (Fig. 8) is in phase with the elastic angular distribution indicating that the parity of this state is positive rather than negative as was previously suggested.⁶

Third, no states in Y^{89} were excited in the region of excitation between 3.1 and 3.7 MeV (see Fig. 3).

Fourth, the angular distributions for the hitherto unreported states at 3.70 ± 0.02 MeV, 3.98 ± 0.02 MeV, and 4.17 ± 0.03 MeV (Fig. 9) allowed the assignment of parities to these states, assuming that they are excited by a single excitation process. The state at 3.70 MeV may be a doublet, since the peak in the energy spectrum was consistently wider than the elastic peak, in which case both states have the same parity; from the sharp structure of the angular distribution it is surmised that the angular momentum transfer involved in the transition to each state is the same.

The shapes of the angular distributions for the 1.51-, 1.75-, 2.22-, and 3.1-MeV states in Y^{89} and the 1.84- and 2.74-MeV states in Sr^{88} are as would be expected from the phase rule and the parities previously assigned.^{6,8,24} Also, peaks consistently appeared in the $Y^{89}(\alpha, \alpha')$ spectra corresponding to excitation energies

of 4.31 ± 0.03 MeV, 4.47 ± 0.03 MeV, and 4.58 ± 0.04 MeV, but consistent angular distributions could not be extracted for these states. A level diagram giving the positions, spins, and parities of the low-lying states in Sr^{88} and Y^{89} is shown in Fig. 10.

IV. DATA ANALYSIS

Fits for the experimental elastic angular distributions for Sr^{88} and Y^{89} were calculated by a parametrized phase-shift analysis.²⁵ The partial-wave expansion for the elastic-scattering amplitude for a spin-zero pro-

TABLE I. Center-of-mass elastic scattering differential cross sections divided by the Rutherford cross section for 42-MeV α particles scattered from Sr^{88} . The quoted uncertainties are relative only.

| $Sr^{88}(\alpha, \alpha), Q=0$ MeV | | | $Y^{89}(\alpha, \alpha), Q=0$ MeV | | |
|------------------------------------|-------------------|-----------|-----------------------------------|-------------------|-----------|
| $\theta_{c.m.}$ | σ/σ_R | Error (%) | $\theta_{c.m.}$ | σ/σ_R | Error (%) |
| 13.3 | 0.709 | 2.0 | 12.5 | 0.858 | 0.57 |
| 14.3 | 0.677 | 2.0 | 13.5 | 0.743 | 0.57 |
| 15.3 | 0.681 | 1.5 | 14.6 | 0.668 | 0.36 |
| 16.4 | 0.659 | 1.5 | 15.6 | 0.680 | 0.56 |
| 17.4 | 0.571 | 1.0 | 16.7 | 0.662 | 0.72 |
| 18.5 | 0.468 | 1.0 | 17.7 | 0.632 | 0.35 |
| 19.5 | 0.330 | 1.0 | 18.8 | 0.523 | 0.58 |
| 20.6 | 0.290 | 1.0 | 19.8 | 0.406 | 0.65 |
| 21.7 | 0.278 | 1.0 | 20.9 | 0.319 | 0.38 |
| 22.7 | 0.307 | 1.0 | 21.9 | 0.276 | 0.58 |
| 23.7 | 0.330 | 1.0 | 23.0 | 0.276 | 0.38 |
| 24.8 | 0.336 | 1.0 | 24.0 | 0.301 | 0.34 |
| 25.8 | 0.291 | 1.0 | 25.1 | 0.312 | 0.31 |
| 26.9 | 0.222 | 1.0 | 26.1 | 0.286 | 0.79 |
| 27.9 | 0.148 | 1.0 | 27.1 | 0.246 | 0.39 |
| 28.9 | 0.102 | 1.1 | 29.2 | 0.108 | 0.64 |
| 29.9 | 0.0895 | 1.0 | 30.2 | 0.0879 | 0.64 |
| 31.0 | 0.112 | 1.0 | 31.3 | 0.0873 | 0.53 |
| 32.0 | 0.142 | 1.0 | 33.4 | 0.140 | 0.35 |
| 33.1 | 0.166 | 1.0 | 35.5 | 0.133 | 0.83 |
| 34.1 | 0.167 | 1.0 | 37.5 | 0.0491 | 0.92 |
| 35.2 | 0.137 | 1.0 | 39.6 | 0.0252 | 0.69 |
| 36.2 | 0.0938 | 1.0 | 42.0 | 0.0567 | 0.59 |
| 37.2 | 0.0513 | 1.1 | 42.7 | 0.0661 | 0.58 |
| 39.3 | 0.0278 | 1.6 | 44.0 | 0.0693 | 0.62 |
| 41.4 | 0.0657 | 1.1 | 46.1 | 0.0327 | 0.71 |
| 43.4 | 0.0923 | 1.1 | 48.2 | 0.0057 | 1.10 |
| 45.5 | 0.0593 | 1.5 | 50.2 | 0.0146 | 1.05 |
| 47.6 | 0.0118 | 1.5 | 52.3 | 0.0375 | 0.86 |
| 49.6 | 0.0097 | 4.1 | 53.0 | 0.0423 | 1.10 |
| 51.7 | 0.0442 | 1.7 | 54.0 | 0.0459 | 1.15 |
| 53.8 | 0.0553 | 2.1 | 56.1 | 0.0146 | 1.18 |
| 55.8 | 0.0295 | 2.4 | 58.5 | 0.00067 | 7.6 |
| 57.9 | 0.0030 | 7.7 | 60.2 | 0.00605 | 2.4 |
| 59.9 | 0.0045 | 7.7 | 62.3 | 0.0213 | 0.96 |
| 62.3 | 0.0248 | 2.1 | 64.3 | 0.0279 | 0.95 |
| 64.3 | 0.0381 | 2.0 | 66.3 | 0.0164 | 1.19 |
| 66.4 | 0.0190 | 2.7 | 68.4 | 0.00325 | 2.40 |
| 68.1 | 0.0039 | 10.8 | 70.4 | 0.00132 | 1.70 |
| 70.1 | 0.0019 | 14.4 | 72.4 | 0.00765 | 1.28 |
| 72.5 | 0.0089 | 4.6 | 74.5 | 0.0133 | 1.62 |
| 74.5 | 0.0147 | 3.0 | 76.5 | 0.0117 | 2.9 |
| 76.5 | 0.0127 | 2.9 | 78.5 | 0.00484 | 4.3 |
| 78.6 | 0.0051 | 3.9 | 80.5 | 0.00072 | 7.6 |
| 80.6 | 0.00094 | 9.5 | 82.5 | 0.00154 | 8.0 |
| 82.6 | 0.0023 | 6.4 | 84.6 | 0.00499 | 4.7 |
| 84.6 | 0.0078 | 6.2 | 86.6 | 0.00603 | 4.5 |

²⁴ *Nuclear Data Tables*, compiled by K. Way *et al.* (Printing and Publishing Office, National Academy of Sciences-National Research Council, Washington 25, D. C., 1960), NRC 61-3-51.

²⁵ J. A. McIntyre, K. H. Wang, and L. C. Becker, *Phys. Rev.* **117**, 1337 (1960); J. Alster and H. E. Conzett, *ibid.* **136**, B1023 (1964); J. Alster and H. E. Conzett, *ibid.* **139**, B50 (1965).

TABLE II. Values of the parameters l_A , Δl_A , δ_0 , l_δ , and Δl_δ used in fitting the parametrized phase-shift analysis to the differential cross sections for the elastic scattering from Sr⁸⁸ and Y⁸⁹.

| | l_A | Δl_A | δ_0 | l_δ | Δl_δ |
|------------------|-------|--------------|------------|------------|-------------------|
| Sr ⁸⁸ | 18.6 | 0.750 | 0.400 | 19.6 | 0.740 |
| Y ⁸⁹ | 18.3 | 0.750 | 0.440 | 19.3 | 0.786 |

jectile scattered by a spin-zero target is

$$f_{el}(\theta) = \frac{1}{2ik} \sum_{l=0}^{\infty} (2l+1)(1 - \eta_l e^{2i\sigma_l}) P_l(\cos\theta), \quad (2)$$

where

$$\sigma_l = \arg\Gamma(1+l+in). \quad (3)$$

It is convenient to write the partial-wave coefficients η_l in terms of two real quantities A_l and δ_l as

$$\eta_l = A_l e^{2i\delta_l}. \quad (4)$$

These quantities are parametrized as

$$A_l = \{1 + \exp[(l_A - l)/\Delta l_A]\}^{-1} \quad (5a)$$

and

$$\delta_l = \delta_0 \{1 + \exp[(l - l_\delta)/\Delta l_\delta]\}^{-1}. \quad (5b)$$

The five parameters l_A , Δl_A , δ_0 , l_δ , and Δl_δ were varied using an automatic search program²⁶ to give the best agreement with the experimental elastic angular distributions. Comparisons of the theoretical and experimental elastic angular distributions for Sr⁸⁸ and Y⁸⁹ are shown in Fig. 4 along with an optical-model angular distribution²⁷ which used a real depth of 50 MeV, an

TABLE III. The spectroscopic parameters deduced from this experiment. Column 2 gives the Q value of the levels in Sr⁸⁸ and Y⁸⁹, column 3 gives the spin and parity, column 4 gives the orbital angular momentum transfer, column 5 gives the $(\beta_I R)^2$ value found by a comparison of the experimental data with the Austern-Blair model, column 6 gives the value of $(\beta_I R)$, and column 7 gives the transition strength in Weisskopf single-particle units calculated with the formula given in the text.

| | Q (MeV) | J^π | I | $(\beta_I R)^2$ (F ²) | $\beta_I R$ (F) | G |
|------------------|--------------|-------------------|--------|--------------------------------------|--------------------|------|
| Sr ⁸⁸ | -1.84 | 2 ⁺ | 2 | 0.25 ± 0.03 | 0.50 | 5.0 |
| | -2.74 | 3 ⁻ | 3 | 0.30 ± 0.04 | 0.55 | 6.2 |
| | -3.21 | 2 ⁺ | | ~0.02 | ~0.14 | ~0.4 |
| Y ⁸⁹ | -0.906 | $\frac{9}{2}^+$ | 5 | 0.010 ± 0.003 | 0.10 | 0.25 |
| | -1.51 | $\frac{3}{2}^+$ | 2 | 0.020 ± 0.004 | 0.14 | 0.42 |
| | -1.75 | $\frac{5}{2}^-$ | 2 | 0.040 ± 0.008 | 0.20 | 0.84 |
| | -2.22 | $(\frac{5}{2})^+$ | 3 | 0.070 ± 0.009 | 0.26 | 1.47 |
| | -2.53 | $(\frac{7}{2})^+$ | 3 | 0.110 ± 0.013 | 0.33 | 2.32 |
| | -2.84 | ? ⁺ | (3) | 0.060 ± 0.006 | 0.24 | 1.27 |
| | -3.1 | ? ⁻ | 2 or 4 | 0.025 ± 0.003 | 0.16 | 0.53 |
| | -3.70 | ? ⁺ | (3) | 0.040 ± 0.006 | 0.19 | 1.0 |
| | -3.98 | ? ⁻ | (2) | 0.030 ± 0.005 | 0.17 | 0.51 |
| | -4.17 | ? ⁻ | (2) | 0.030 ± 0.005 | 0.17 | 0.51 |

²⁶ A copy of the computer program may be obtained from J. Alster.

²⁷ The coupled-channel calculation computer code of J. G. Wills, Ph.D. thesis, University of Washington, 1963 (unpublished), was used.

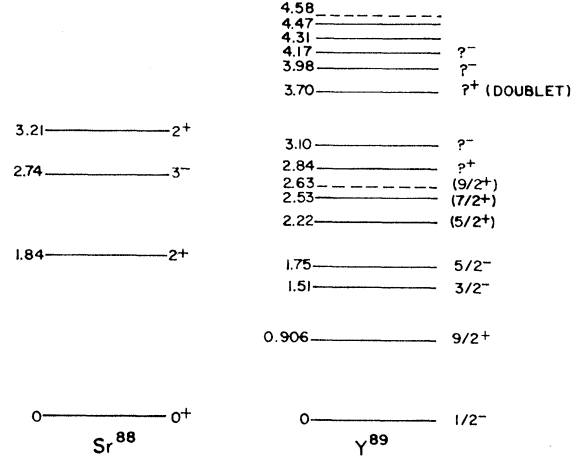


FIG. 10. Energy level diagrams showing positions, spins, and parities of the low-lying states of Sr⁸⁸ and Y⁸⁹. The energies and spins of the states of Y⁸⁸ up to 2.84 MeV are taken from Ref. 6. The spin and parity of the 3.21-MeV state of Sr⁸⁸ is obtained from Ref. 8.

imaginary depth of 20 MeV, a radius of 7.036 F and a diffuseness of 0.50 F. Table II gives the values of the five parameters l_A , Δl_A , δ_0 , l_δ , and Δl_δ for Sr⁸⁸ and Y⁸⁹. The fits are fairly good for angles smaller than 65 deg.

Inelastic differential cross sections were calculated using the adiabatic approximation of Austern and Blair,²⁸ which relates the inelastic-scattering amplitudes to the partial derivatives of the partial-wave coefficients calculated for elastic scattering. The single excitation scattering amplitude for a transition involving angular momentum I , projection M , is given by

$$f_{I,M}(\theta) = \frac{-i}{2} \beta_I R \sum_{l,l'} i^{l-l'} (2l'+1)^{1/2} \times \exp[i(\sigma_l + \sigma_{l'})] \langle l' I 0 0 | l I - M M | l 0 \rangle \times \frac{\partial \eta_l}{\partial \bar{l}} Y_{\nu}^{-M}(\theta, 0), \quad (6)$$

where \bar{l} is an average orbital angular momentum defined by $\bar{l} \equiv (l+l')/2$ and $\beta_I R$ is the collective parameter giving the strength of the transition. Other than the normalization parameter $(\beta_I R)^2$ there are no free parameters in the calculation of the inelastic angular distributions, since the partial-wave coefficients $1 - \eta_l$ are obtained from the experimental elastic angular distribution. The calculation is normalized to the experiment in that region of the angular distribution where the elastic fit is good, i.e., for angles smaller than 50 deg. Uncertainties in the values of $(\beta_I R)^2$ were estimated by finding the extreme credible fits in this angular region. The failure of the fits at larger angles is to be expected in view of the fact that no good fit could be found in that region for the elastic scattering.

²⁸ N. Austern and J. S. Blair, Ann. Phys. (N. Y.) 33, 15 (1965).

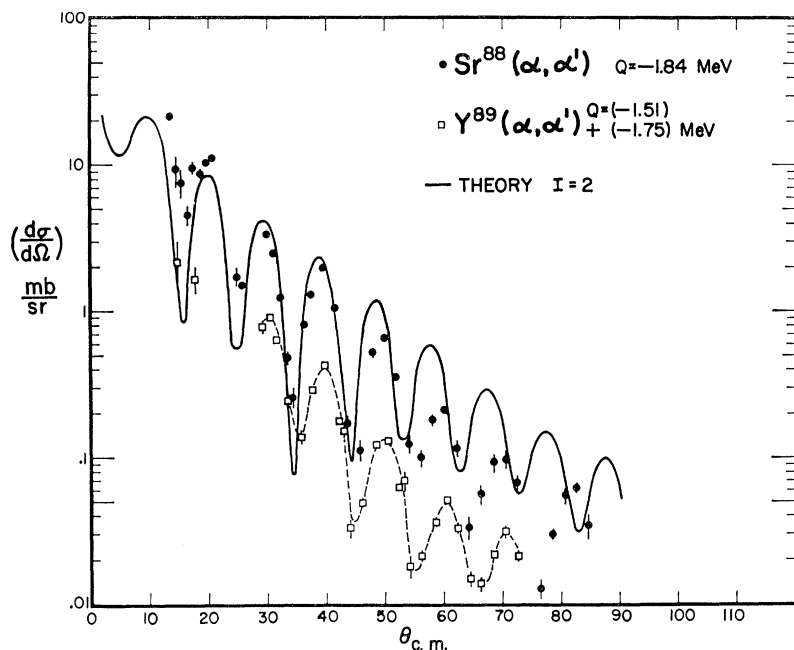


FIG. 11. Comparison of the Austern-Blair adiabatic approximation for an $I=2$ transition to the angular distribution for the excitation of the 1.84-MeV state of Sr^{88} . The theoretical curve is normalized by averaging over the first three maxima in the angular distribution (up to 45 deg). The sum of the differential cross sections for the 1.51- and 1.75-MeV states in Y^{89} is shown for comparison. The dashed curve is only to guide the eye.

Figure 11 shows the fit obtained for the 1.84-MeV state in Sr^{88} and the sum of the differential cross sections for the 1.51- and 1.75-MeV states in Y^{89} for an $I=2$ transition. Figure 12 shows the fit to the 2.74-MeV state in Sr^{88} and the sum of the 2.22-, 2.53-, and 2.84-MeV states in Y^{89} for an $I=3$ transition. Figure 13 shows the angular distribution to the $g_{9/2}$ single-particle state in Y^{89} and the fit obtained using an $I=5$ transition. Table III gives the spins, parities, angular momentum transfer, and the extracted values of $(\beta_I R)^2$,

and the transition strength in Weisskopf units of single-particle transition strength given by the relation

$$G = \frac{B(E_I)}{B_{sp}(I)} = \frac{9}{4\pi} \frac{Z^2}{(2I+1)} \left(\frac{3+I}{3}\right)^2 \frac{(\beta_I R)^2}{(1.2A^{1/3})^2}. \quad (7)$$

The value of the $(\beta_3 R)^2$ for the 2.74-MeV state in Sr^{88} is consistent with the value of β_3 previously measured at this laboratory,¹ and is similar to the value

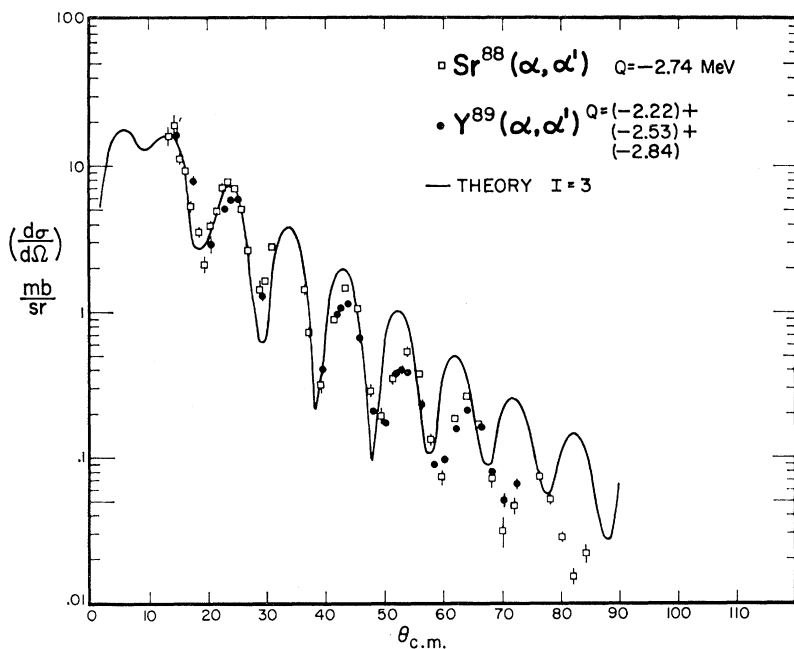


FIG. 12. Comparison of the Austern-Blair adiabatic approximation for an $I=3$ transition to the angular distribution for the excitation of the 2.74-MeV state of Sr^{88} . The theoretical curve is normalized by averaging over the first four maxima in the angular distribution (up to 45 deg). The sum of the differential cross sections for the 2.22-, 2.53-, and 2.84-MeV states in Y^{89} is shown for comparison.

of $\beta_3 R$ for the 3^- state at 2.74 MeV in Zr^{90,29} The value of $(\beta_2 R)^2$ for the 1.84-MeV state is smaller than that extracted from the older data, taken at this laboratory, and also smaller than the value found from a lifetime measurement³⁰ of the 1.84-MeV state. Our value for $\beta_2 R$ is similar to that found for the first 2^+ state in Zr^{90,29}

The values of $(\beta_3 R)^2$ for the 2.22- and 2.53-MeV states in Y⁸⁹ suggest that these states may be collective in nature.

V. DISCUSSION

It is seen from Figs. 11 and 12 and Table III that the predictions of the weak-coupling core-excitation model do not hold for the states in Y⁸⁹. The sum of the values of $(\beta_2 R)^2$ (proportional to $d\sigma/d\Omega$) for the 1.51- and 1.75-MeV states in Y⁸⁹ is about a factor of 4 less than the value of $(\beta_2 R)^2$ for the 1.84-MeV state in Sr⁸⁸ and the sum of the values of $(\beta_3 R)^2$ for the 2.22- and 2.53-MeV states in Y⁸⁹ is only about 60% of the value of $(\beta_3 R)^2$ for the 2.74-MeV state in Sr⁸⁸. The 2.84- and 3.1-MeV states in Y⁸⁹ cannot be members of a doublet corresponding to the 3.21 MeV (2^+) state in Sr⁸⁸ since they have opposite parities as mentioned in the previous section. Also, the ratio of the $(\beta_2 R)^2$ values for the 1.75-MeV state to the value of the $(\beta_2 R)^2$ for the 1.51-MeV state in Y⁸⁹ is 2 instead of 6/4 as predicted by Eq. (1). The ratio of the $(\beta_3 R)^2$ value for the 2.53-MeV state to the $(\beta_3 R)^2$ for the 2.22-MeV state, however, is almost 8/6 as predicted by Eq. (1).

If the values of $(\beta_3 R)^2$ for the three positive parity states (2.22, 2.53, and 2.84 MeV) in Y⁸⁹, are added, their sum is almost equal to the $(\beta_3 R)^2$ value for the 2.74-MeV state in Sr⁸⁸ but the existence of three positive-parity states is not explained by the simple weak-coupling core-excitation model. The existence of the third state might be due to the presence of a single-particle configuration with spin and parity either $\frac{5}{2}^+$ or $\frac{7}{2}^+$ lying close to the core-excitation doublet. The mixing of such a state with the state of like spin could then give rise to two states with comparable transition strengths. If the single-particle state is not strongly excited then one would expect the ratio of the sum of the values of $(\beta_3 R)^2$ for the two mixed states to the value of the $(\beta_3 R)^2$ for the third state to be either 8/6 or 6/8. This is not observed.

From Table III it is seen that the transition strengths G measured in Weisskopf units are not large for any of the positive parity transitions of Sr⁸⁸ or Y⁸⁹ suggesting that collective descriptions are inappropriate for the states in question. An alternative description of the Y⁸⁹ states at 1.51-MeV ($\frac{3}{2}^-$) and 1.75-MeV ($\frac{5}{2}^-$) in terms of simple shell-model configurations was briefly discussed in the Introduction; this description will now be developed more quantitatively.

²⁹ D. L. Hendrie and G. W. Farwell, Phys. Letters 9, 321 (1964); H. W. Broek and J. L. Yntema, Phys. Rev. 138, B334 (1965).
³⁰ S. Ofer and A. Schwarzschild, Phys. Rev. Letters 3, 384 (1959).

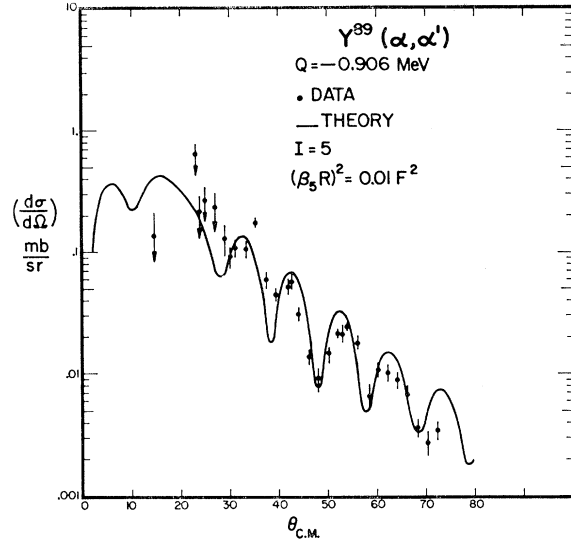


FIG. 13. Comparison of the Austern-Blair adiabatic approximation for an $I=5$ transition to the angular distribution for excitation of the 0.906-MeV state of Y⁸⁹. The theoretical curve is normalized by averaging over the maxima in the angular distribution up to 55 deg.

An energy diagram of the shell-model orbitals pertinent to Sr⁸⁸ is shown in Fig. 14, and those particle-hole configurations which could form a 2^+ seniority two state in Sr⁸⁸ are indicated by arrows joining the particle and hole. The energetics suggest that, of the

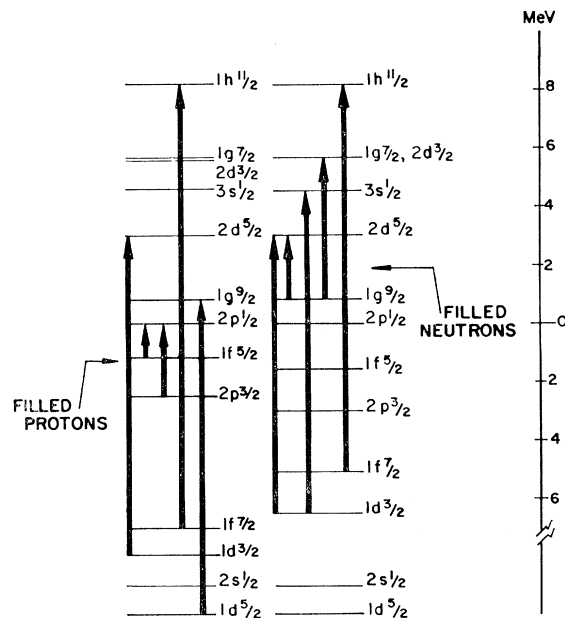


FIG. 14. Single-particle transitions that can form a 2^+ state in Sr⁸⁸. The neutron energy spacings are taken from B. L. Cohen, R. H. Fulmer, A. L. McCarthy, and P. Mukherjee, Rev. Mod. Phys. 35, 332 (1963), and the proton energy spacings from D. D. Armstrong and A. G. Blair, Phys. Rev. 140, B1226 (1965). Where no proton energy spacings were available they were assumed to be the same as the neutron spacings. The energy scale has been drastically compressed below the $1f_{7/2}$ subshell.

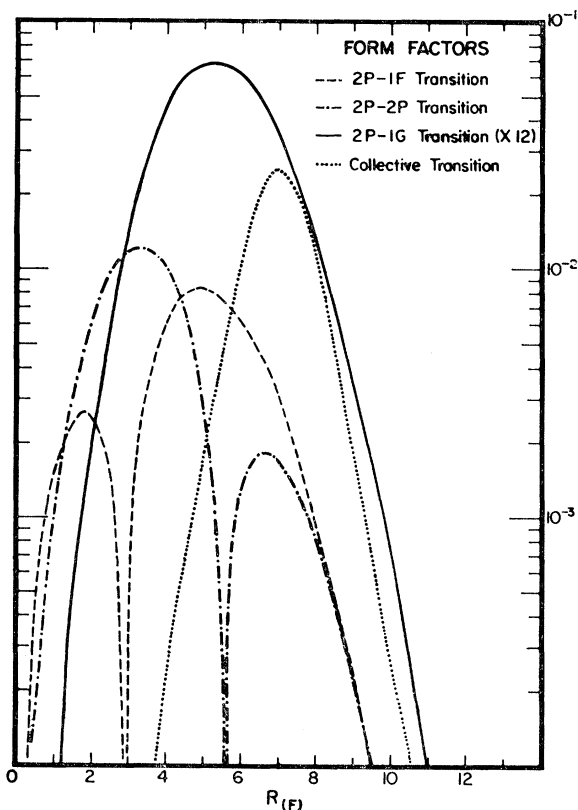


FIG. 15. Comparison of the single-particle form factors for the $2p-1f$, $2p-2p$, and $2p-1g$ transitions in Y^{89} . The form factors are actually negative at small radii. The collective derivative form factor is also shown.

proton configurations, only the $2p_{1/2}-2\bar{p}_{3/2}$ and $2p_{1/2}-1\bar{f}_{5/2}$ configurations will be important and similarly that the $d_{5/2}-\bar{g}_{9/2}$ configuration is the most important of the neutron configurations. It is also seen that the configurations of Y^{89} in which there are either a $2p_{3/2}$ or a $1f_{5/2}$ hole in the Zr^{90} ground state should not lie more than two MeV above the ground state.

As a definite model we shall assume that the ground state of Sr^{88} is the closed shell,

$$|0^+\rangle = |(p_{3/2})^4, (f_{5/2})^6\rangle. \quad (8a)$$

For reasons of simplicity, and because no experimental evidence is available on the matter, we shall make the crucial assumption that neutron configurations are unimportant in the low-lying 2^+ states of Sr^{88} so that the wave functions of these states contain only proton configurations,

$$\langle 2^+ | = P \langle p_{1/2}, \bar{p}_{3/2} | + (1-P^2)^{1/2} \langle p_{1/2}, \bar{f}_{5/2} | \quad (8b)$$

and

$$\langle 2^{+'} | = (1-P^2)^{1/2} \langle p_{1/2}, \bar{p}_{3/2} | - P \langle p_{1/2}, \bar{f}_{5/2} |, \quad (8c)$$

where P is a mixing parameter whose value will be determined by the observed inelastic differential cross sections in Sr^{88} . The ground state of Y^{89} is taken to be

the single-particle configuration

$$|\frac{1}{2}^-\rangle = |2p_{1/2}, (2p_{3/2})^4, (1f_{5/2})^6\rangle \quad (9a)$$

and, for the moment, the third and fourth states of Y^{89} are assumed to have the proton configurations

$$\langle \frac{3}{2}^- | = \langle (2p_{1/2})^2, 2\bar{p}_{3/2} |, \quad (9b)$$

$$\langle \frac{5}{2}^- | = \langle (2p_{1/2})^2, 1\bar{f}_{5/2} |. \quad (9c)$$

An interaction potential between the incident alpha particle and the target protons will induce nuclear transitions between these states. Recently, DWBA calculations which utilize such a single-particle description of the nucleus have been compared to inelastic proton-scattering experiments.³¹ The details of an analogous calculation, suitably modified for the scattering of alpha particles from Sr^{88} and Y^{89} , are given in the Appendix.

Using the model wave functions [Eqs. (8) and (9)] and the DWBA formalism for inelastic cross sections [Eq. (A1)], we find a simple sum rule relating the cal-

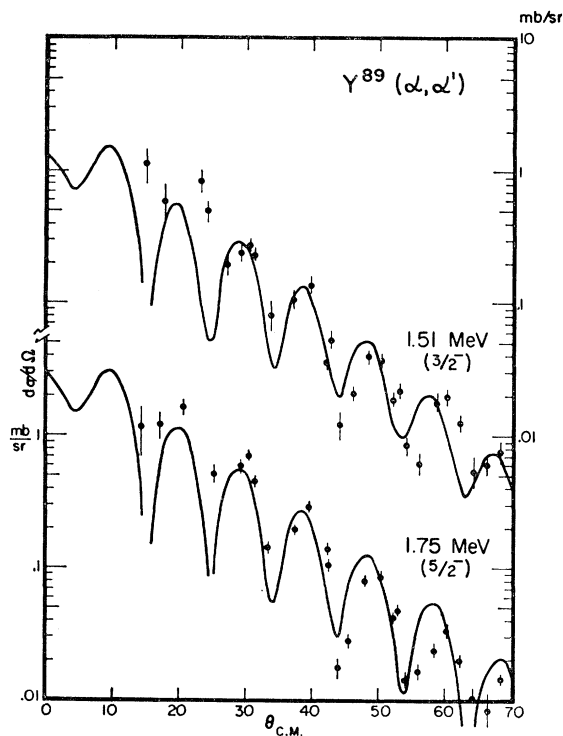


FIG. 16. Comparison of the predictions of the DWBA calculations for the single particle $2p_{1/2} \rightarrow 2p_{3/2}$ and $2p_{1/2} \rightarrow 1f_{5/2}$ transitions to the differential cross sections for the excitation of the 1.51-MeV ($\frac{3}{2}^-$) and 1.75-MeV ($\frac{5}{2}^-$) states of Y^{89} . The relative magnitudes of the predicted angular distributions, R , is fixed by the choice of the parameters $\gamma=0.50 \text{ F}^{-1}$ and $a=2.20 \text{ F}$. The normalization of the absolute magnitudes of the predicted angular distributions is arbitrary.

³¹ H. O. Funsten, N. R. Roberson, and E. Rost, Phys. Rev. **134**, B117 (1964).

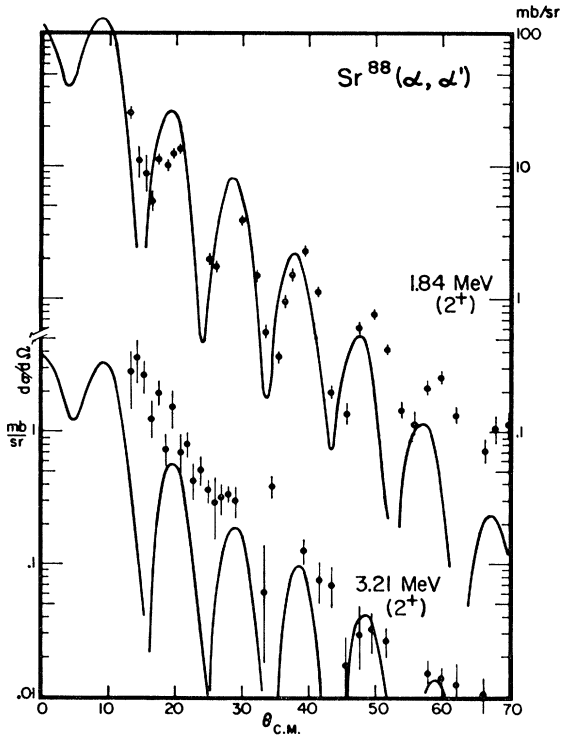


FIG. 17. Comparison of the predictions of the DWBA calculations for the single-particle transitions forming the mixed configuration 2^+ states to the differential cross sections for the excitation of the 1.84- and 3.21-MeV states in Sr⁸⁸. The mixing parameter P (see text) was adjusted to give the correct ratio between the predicted angular distributions. The normalization of the absolute magnitudes of the predicted angular distributions is arbitrary.

culated differential cross sections for inelastic scattering from Sr⁸⁸ and Y⁸⁹.

$$\frac{d\sigma}{d\Omega}(2^+) + \frac{d\sigma}{d\Omega}(2^+) = 2 \left[\frac{d\sigma}{d\Omega}(\frac{3}{2}^-) + \frac{d\sigma}{d\Omega}(\frac{5}{2}^-) \right]. \quad (10)$$

As is seen from Table III, this relation is closer to the experimental results than is the weak-coupling core-excitation prediction.

However, it is known that the ground state of Zr⁹⁰ contains appreciable mixing of the nearly degenerate $(2p_{1/2})^2$ and $(g_{9/2})^2$ proton configurations, with a ground state¹⁵⁻¹⁷

$$|0^+\rangle = A |(\dot{p}_{1/2})^2\rangle + (1-A^2)^{1/2} |(g_{9/2})^2\rangle. \quad (11)$$

The mixing parameter A has been measured to be about 0.8. In view of this we might expect that the most important admixtures to the $\frac{3}{2}^-$ and $\frac{5}{2}^-$ excited states of Y⁸⁹ involve the paired $g_{9/2}$ orbitals, so that their wave functions become

$$\langle \frac{3}{2}^- | = B \langle (\dot{p}_{1/2})^2, \bar{p}_{3/2} | + (1-B^2)^{1/2} \langle (g_{9/2})^2, \bar{p}_{3/2} |, \quad (12a)$$

$$\langle \frac{5}{2}^- | = C \langle (\dot{p}_{1/2})^2, \bar{f}_{5/2} | + (1-C^2)^{1/2} \langle (g_{9/2})^2, \bar{f}_{5/2} |. \quad (12b)$$

The Y⁸⁹ inelastic alpha-particle cross sections to these states would then be expected to be decreased by factors B^2 and C^2 , respectively. Using the same mixing

($A=B=C$) as is found for Zr⁹⁰, the sum of the Sr⁸⁸ cross sections [Eq. (10)] is expected to be about 3.1 times the sum of the two Y⁸⁹ cross sections, a value still nearer the experimental factor of 4.

Another quantity that can be calculated with this model is the ratio R of the cross sections to the 1.75-MeV ($\frac{5}{2}^-$) and 1.51-MeV ($\frac{3}{2}^-$) states of Y⁸⁹. The weak-coupling model predicts this ratio to be 6/4, as would our single-particle model were the radial matrix elements for the $2p-2p$ and $1f-2p$ transitions identical. However, Fig. 15 shows that the $2p-2p$ radial form factor is smaller than the $1f-2p$ form factor. This should be reflected in a relatively smaller cross section to the $\frac{3}{2}^-$ state.

Detailed integrations to form the cross sections have been performed as outlined in the Appendix. A Gaussian interaction between the alpha particle and the proton was adopted and simple harmonic oscillator wave functions were used for the proton orbitals. Computations were performed for several sets of values for the Gaussian range and the oscillator length.³² All reasonable values of the parameters gave almost identical shapes for the calculated differential cross sections, and ratios R ranging between 1.8 and 2.5, in agreement with the measured ratio of 2.0. Figure 16 shows the comparison between the calculated single-particle cross sections and the data for excitation of the 1.51-MeV ($\frac{3}{2}^-$) and 1.75-MeV ($\frac{5}{2}^-$) states of Y⁸⁹. The absolute normalization of the calculations is arbitrary, but the ratio R for the two cross sections is determined once the Gaussian range and oscillator length are chosen. It should be noted that the shape of the single-particle cross sections is very similar to the usual collective cross sections, as has previously been suggested.³² Comparison to Fig. 11 shows that the detailed agreement to the data is actually better using the single-particle calculation than with the collective adiabatic calculation.

This calculation was repeated with the same parameters for the mixed configuration 2^+ states of Sr⁸⁸. A value of the mixing parameter $P=1/\sqrt{2}$ was found to give reasonable agreement for the relative cross sections to the 1.84-MeV (2^+) and 3.21-MeV (2^+) states of Sr⁸⁸. The comparison to the data is shown in Fig. 17. In spite of the poor quality of the data for the 3.21-MeV state, the value of P is fairly well determined due to the sensitivity of the interference seen from Eq. (8). The radial form factors used to calculate these cross sections are shown in Fig. 18. The 1.84-MeV (2^+) form factor is quite similar to the collective form factor in the nuclear tail, but the 3.21-MeV (2^+) form factor bears no resemblance to the collective form factor. Nevertheless, Fig. 17 shows that reasonable shapes for the differential cross sections are calculated in each case.

Using the value of the Gaussian strength V_G for the alpha-particle-proton potential that is determined from

³² D. Jackson, Phys. Letters 14, 118 (1965).

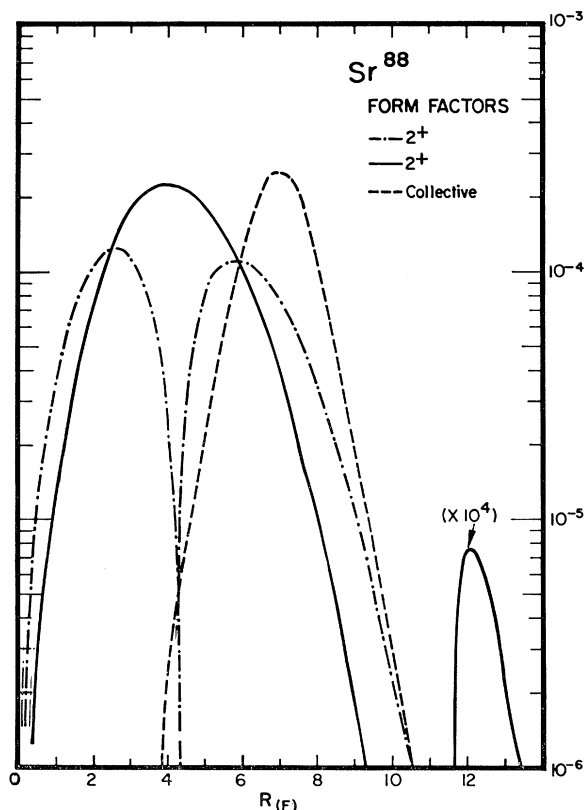


FIG. 18. Comparison of the single-particle form factors for the transitions forming the mixed configuration 2^+ states with the collective form factor for Sr^{88} . These radial form factors are actually negative at small radii, but are shown as positive on a logarithmic scale. The right-hand curve has been multiplied by 10^4 .

the magnitude of the cross section to the $g_{9/2}$ single-particle state (see Appendix) we can calculate the absolute magnitudes of the cross sections to the 1.84-MeV (2^+) and 3.21-MeV (2^+) states of Sr^{88} and to the 1.51-MeV ($\frac{3}{2}^-$) and 1.75-MeV ($\frac{5}{2}^-$) states of Y^{89} . The calculated angular distributions for Y^{89} are approximately a factor of 5 smaller than the experimental differential cross sections. This discrepancy certainly constitutes a major problem with this single-particle interpretation. This normalization hinges upon the value of $\beta_5 R$ extracted from the $2p_{1/2}-1g_{9/2}$ transition. The Austern-Blair model is not expected to be accurate for this large an angular momentum transfer,²⁸ but the value of $(\beta_5 R)^2$ is not expected to be in error by as much as a factor of 5.

The magnitudes of the cross sections can be enhanced by inclusion of neglected configurations, particularly the neutron particle-hole configurations, but then the simplicity of the present model is lost. Investigations of the reaction, $\text{Y}^{89}(d, \text{He}^3)\text{Sr}^{88}$ and $\text{Zr}^{90}(d, \text{He}^3)\text{Y}^{98}$ are being performed in this laboratory to study further the single-particle properties of these nuclei.³³ Preliminary

³³ C. D. Kavaloski, J. Lilley, D. C. Shreve, and N. Stein (private communication).

results indicate that the 1.51- and 1.75-MeV states of Y^{89} do have a large single hole strength. Further, it is found that the 1.84- and 3.21-MeV states of Sr^{88} have a large single hole strength, and in addition seem to have quite similar differential cross sections. These results are in qualitative agreement with the single-particle model discussed here.

VI. CONCLUSIONS

There are several conclusions that can be drawn from this experiment. First, the Austern-Blair model, using the partial-wave amplitudes obtained from the parametrized phase-shift calculation for the elastic angular distribution, gives good agreement to the experimental inelastic angular distributions for angles less than 65 deg. It is seen, however, that the quality of the fit for the inelastic angular distributions is dependent on the fit obtained for the elastic angular distribution. The calculated inelastic angular distributions start to fall out of phase with the data at large angles ($\theta > 65$ deg) in much the same way that the parametrized phase-shift calculation did for the elastic scattering.

Second, the angular distribution for the $g_{9/2}$ (0.906-MeV) single-particle state in Y^{89} is very similar to those for collective states. In fact, the angular distribution calculated using the adiabatic collective model is in reasonable agreement with the data, and the magnitude of $\beta_5 R$ obtained in this manner agrees with an estimate made for a single-particle transition.³² It was also shown in Sec. V that the shapes of the angular distributions calculated for an $I=2$ transition using single-particle wave functions are almost identical to those calculated using collective models. These experimental and theoretical results verify the belief³² that the shapes of the angular distributions for inelastic scattering are relatively insensitive to the nature of the excited state.

Third, it was shown that the weak-coupling core-excitation model is not a complete description of the 2.22-MeV ($\frac{5}{2}^+$) and 2.53-MeV ($\frac{7}{2}^+$) states in Y^{89} and is not at all valid for the 1.51-MeV ($\frac{3}{2}^-$) and 1.75-MeV ($\frac{5}{2}^-$) states or the 2.84- and 3.1-MeV states. The sum of the differential cross sections for the 1.51- and 1.75-MeV states in Y^{89} was a factor of 4 too small compared to the 1.84-MeV (2^+) state in Sr^{88} and the 2.84-MeV state of Y^{89} had the wrong parity to be related to the 3.21-MeV (2^+) state of Sr^{88} . The explanation of three positive parity states in Y^{89} corresponding to the mixing of a single-particle state with one of the core-excitation states given in Sec. V is somewhat dubious.

Fourth, calculations made using simple shell-model configurations, predicted that the ratio of the sum of the differential cross sections for the 1.84-MeV (2^+) and 3.21-MeV (2^+) states in Sr^{88} to the sum of the differential cross sections for the 1.51-MeV ($\frac{3}{2}^-$) and 1.75-MeV ($\frac{5}{2}^-$) states in Y^{89} should be two. With the inclusion of some $(g_{9/2})^2$ configuration mixing in the excited states

of Y⁸⁹ the calculated ratio becomes 3.1, a value which is approaching the observed ratio of approximately four. The calculated ratio of the cross sections leading to the 1.75- and 1.51-MeV states in Y⁸⁹ was found to be in agreement with the experimental results. The absolute magnitudes of the differential cross sections calculated using these simple configurations, however, were lower than the experimental values by a factor of 5. These results suggest that the states of Y⁸⁹ and Sr⁸⁸ in question contain more complicated configurations than were assumed and indicate the need of further experimental and theoretical investigations.

ACKNOWLEDGMENTS

It is a pleasure to thank Dr. J. S. Blair for his continued interest in this work and for his criticism of the manuscript, Dr. S. M. Shafroth and Dr. A. S. Reiner for helpful discussions, and Dr. G. W. Farwell for his encouragement. Thanks are due to F. Karasek for sending us a Y foil and to Mrs. J. Sauer for the preparation of the Sr target.

APPENDIX

The DWBA expression for the differential cross section for angular momentum transfer I can be written as³¹

$$\frac{d\sigma}{d\Omega} = \frac{k_f}{k_i} \left(\frac{\mu}{2\pi\hbar} \right)^2 \frac{(2J_f+1)}{(2J_i+1)(2I+1)} \times \sum_m \left| \int d^3R \chi_f^{(-)*}(\mathbf{k}_f, \mathbf{R}) F_I(R) [i^I Y_I^m(\hat{R})] \times \chi_i^{(+)}(\mathbf{k}_i, \mathbf{R}) \right|^2, \quad (\text{A1})$$

where μ is the reduced mass and J_i and J_f are the initial and final nuclear spins. The projectile wave functions χ_i and χ_f are generated from the optical model used to fit the elastic angular distribution.^{27,34}

For a collective transition the form factor is³¹

$$F_I(R) = -(2I+1)^{-1/2} \beta_I R_0 (dU/dR), \quad (\text{A2})$$

where U is the optical potential and the collective parameter β_I is related to the restoring force parameter C_I by

$$\beta_I^2 = (2I+1)(\hbar\omega_I/2C_I). \quad (\text{A3})$$

A single-particle transition within the target nucleus can be induced by a central two-body potential between the coordinate ξ_i of the relevant nucleon and the coordinate \mathbf{R} of the projectile. A central potential of

Gaussian form is chosen

$$V = \sum_{i=1}^n V(\mathbf{R}-\xi_i) = V_G \sum_{i=1}^n \exp[-\gamma^2 |\mathbf{R}-\xi_i|^2] \quad (\text{A4})$$

and expanded into multipoles

$$\exp[-\gamma^2 |\mathbf{R}-\xi_i|^2] = 4\pi \sum_{\lambda\mu} i^\lambda j_\lambda(-2i\gamma^2 R\xi_i) \times \exp[-\gamma^2(R^2+\xi_i^2)] Y_{\lambda\mu}(\hat{\xi}_i) Y_{\lambda\mu}^*(\hat{R}). \quad (\text{A5})$$

We generalize Ref. 31, and separate the form factor for this single-particle transition into angular and radial integrations

$$F_I(R) = 4\pi V_G M_I \mathcal{G}_I(R),$$

where

$$M_I = (2J_f+1)^{1/2} \sum_{\mu M_i} \begin{pmatrix} l & J_i & J_f \\ \mu & M_i & -M_f \end{pmatrix} \times \langle J_f M_f | \sum_{i=1}^n Y_{l\mu}(\hat{\xi}_i) | J_i M_i \rangle \quad (\text{A6})$$

and

$$\mathcal{G}_I(R) = (-)^I e^{-\gamma^2 R^2} \int d\xi \xi^2 j_I(-2i\gamma^2 R\xi) e^{-\gamma^2 \xi^2} u_i(\xi) u_f(\xi).$$

These radial form factors, $\mathcal{G}_I(R)$, are the same for a given single-particle transition in both Sr⁸⁸ and Y⁸⁹. The initial and final nuclear wave functions u_i and u_f are taken to be for a nucleon moving in a harmonic oscillator well. These wave functions are written as $u(\xi) \sim \exp(-\xi^2/2a^2)$, with a being the usual length parameter. A value of $a=2.20$ F is used in the present work. Shell-model calculations for the spectra of Zr⁹⁰ have used the value $a=2.30$ F.¹⁶

The range γ of the Gaussian potential between the alpha particle and the nucleon has been estimated to range from 0.45 F⁻¹ to 0.56 F⁻¹; a value of $\gamma=0.50$ F⁻¹ is used in this work. The strength V_G is near 50 MeV.^{32,35}

Projectile wave functions obtained from the optical potential are integrated with the radial form factors using a slightly modified version of a computer code due to Wills.²⁷ It is found that the locations of the oscillations in the $L=2$ differential cross sections are not dependent on the parameters or configurations, provided only that the slopes in the outer regions of the form factors are similar to that of the derivative form factor. This confirms the assumption made in Ref. 32. The relative magnitudes of the maxima of the oscillations can be slightly altered by changing the parameters, particularly the oscillator length, and the over-all magnitude of the cross sections is strongly dependent on the parameters a and γ .

The radial form factor $\mathcal{G}_I(R)$ can be evaluated by expanding the spherical Bessel function and performing

³⁴ R. H. Bassell, R. M. Drisko, and G. R. Satchler, Oak Ridge National Laboratory Report No. ORNL-3240, 1962 (unpublished).

³⁵ S. Sack, L. C. Biedenharn, and G. Breit, Phys. Rev. **93**, 321 (1954).

the integration. For the $L=2$ transitions we have

$$g_2(R) = -\frac{e^{-\alpha^2 R^2}}{a^9 b^9} (2/7)^{1/2} \left\{ \frac{4}{15} \frac{\gamma^{12} R^6}{b^6} + \frac{2}{15} \frac{\gamma^8}{b^4} (18 - 5a^2 b^2) R^4 + \frac{\gamma^4}{15 b^2} (63 - 35a^2 b^2) R^2 \right\} \quad (\text{A7})$$

for the $1f \rightarrow 2p$ transition,

$$g_2(R) = -\frac{e^{-\alpha^2 R^2}}{a^9 b^9} \left\{ \frac{4}{15} \frac{\gamma^{12} R^6}{b^6} + \frac{4}{15} \frac{\gamma^8}{b^4} (7 - 5a^2 b^2) R^4 + \frac{1}{15} \frac{\gamma^4}{b^2} (63 - 90a^2 b^2 + 25a^4 b^4) R^2 \right\} \quad (\text{A8})$$

for the $2p \rightarrow 2p$ transition, and

$$g_5(R) = \frac{32e^{-\alpha^2 R^2}}{(45\sqrt{7})a^{10}b^{10}} \times \left\{ \frac{1}{4} \frac{\gamma^{14} R^7}{b^7} + \frac{1}{8} \frac{\gamma^{10}}{b^5} (13 - 5a^2 b^2) R^5 \right\} \quad (\text{A9})$$

for the $2p \rightarrow 1g$ $L=5$ transition. To simplify the above equations the parameters $b^2 = \gamma^2 + 1/a^2$ and $\alpha^2 = \gamma^2 - \gamma^4/b^2$ have been introduced.

The angular matrix elements for promotion into an unfilled shell are³⁶

$$M_I = (n)^{1/2} \left[\frac{(2J_i + 1)(2j_f + 1)(2I + 1)(2j_i + 1)}{4\pi} \right]^{1/2} \begin{pmatrix} j_f & I & j_i \\ -\frac{1}{2} & 0 & \frac{1}{2} \end{pmatrix} \times \sum_{J_1 V_1} [j_i^{n-1}(V_1 J_1) j_i, J_i | \{ j_i^n V_i J_i \}] (-)^{j_i + j_f + J_f + I + J_1 - 1/2} \begin{Bmatrix} j_f & j_i & I \\ J_i & J_f & J_1 \end{Bmatrix}, \quad (\text{A10})$$

where there are initially n particles in the j_i shell, and one is promoted to the j_f shell. The sum is over intermediate spin and seniority. In Y^{89} the valence proton already in the $2p_{1/2}$ subshell blocks some of the promotions into this state, and Eq. (A10) cannot be used directly. The angular integrals are

$$\begin{aligned} \text{Sr}^{88}: \quad & |M_{pp}|^2 = 1/5\pi, \\ & |M_{pf}|^2 = 3/10\pi; \\ \text{Y}^{89}: \quad & |M_{p0}|^2 = 1/4\pi, \\ & |M_{pp}|^2 = 1/4\pi, \\ & |M_{pf}|^2 = 1/4\pi. \end{aligned}$$

The DWBA code used here could only be used for $L=2$ transitions. For other multiplicities only comparisons of the form factors can provide ratios of cross sections.³² The collective and single-particle form factors are compared at some radius in the tail region, and an effective $\beta_5 R$ is extracted for the excitation of the

0.906-MeV state of Y^{89} :

$$\beta_5 R = \frac{(\sqrt{11})4\pi V_G M_5 J_5}{dU/dR} \Big|_{R=R_a}. \quad (\text{A11})$$

This is normalized to the experimental value of $\beta_5 R = 0.10$ F, and V_G is determined. Using $a = 2.20$ F and $\gamma = 0.50$ F⁻¹, the V_G 's were determined for $R_a = 8.0$ and 8.5 F. The average of these two determinations of V_G was taken, and the difference was regarded as the uncertainty, providing $V_G = 59 \pm 10$ MeV. This is quite similar to the strength obtained for the free proton-alpha-particle potential.³⁵

A comparison of the $2p$ - $1g$ form factor to the $2p$ - $2p$ and $1f$ - $2p$ form factors confirms the fact that the differential cross sections predicted for the 1.51-MeV ($\frac{3}{2}^-$) and 1.75-MeV ($\frac{5}{2}^-$) states of Y^{89} are about a factor of 5 smaller than are found experimentally.

³⁶ A. de-Shalit and I. Talmi, *Nuclear Shell Theory* (Academic Press Inc., New York, 1963).